Available online at www.sciencedirect.com
SCIENCE DIRECT®

Journal of the European Ceramic Society 24 (2004) 2969–2976

www.elsevier.com/locate/jeurceramsoc

Preparation of $Pb(Zr,Ti)O_3$ thin films by soft chemical route

F.M. Pontes[a], E.R. Leite[a,*], M.S.J. Nunes[a], D.S.L. Pontes[a], E. Longo[a], R. Magnani[a], P.S. Pizani[b], J.A. Varela[c]

[a]*LIEC, CMDMC, Department of Chemistry, UFSCar, Via Washington Luiz, km 235, CP-676, CEP-13565-905, São Carlos, S. P., Brazil*
[b]*Department of Physics, UFSCar, Via Washington Luiz, km 235, CEP-13565-905, São Carlos, S. P., Brazil*
[c]*Institute of Chemistry, UNESP, Araraquara, S. P., Brazil*

Received 17 November 2002; received in revised form 17 April 2003; accepted 27 April 2003

Abstract

Lead zirconate titanate, $Pb(Zr_{0.3}Ti_{0.7})O_3$ (PZT) thin films were prepared with success by the polymeric precursor method. Differential scanning calorimetry (DSC), thermogravimetric analysis (TGA), Fourier-transform infrared spectroscopy (FT-IR), Micro-Raman spectroscopy and X-ray diffraction (XRD) were used to investigate the formation of the PZT perovskite phase. X-ray diffraction revealed that the film showed good crystallinity and no presence of secondary phases was identified. This indicates that the PZT thin films were crystallized in a single phase. PZT thin films showed a well-developed dense grain structure with uniform distribution, without the presence of rosette structure. The Raman spectra undoubtedly revealed these thin films in the tetragonal phase. For the thin films annealed at the 500–700 °C range, the vibration modes of the oxygen sublattice of the PZT perovskite phase were confirmed by FT-IR. The room temperature dielectric constant and dielectric loss of the PZT films, measured at 1 kHz were 646 and 0.090, respectively, for thin film with 365 nm thickness annealed at 700 °C for 2 h. A typical P–E hysteresis loop was observed and the measured values of P_s, P_r and E_c were 68 μC/cm^2, 44 μC/cm^2 and 123 kV/cm, respectively. The leakage current density was about 4.8×10^{-7} A/cm^2 at 1.5 V.

Keywords: Dielectric properties; Films; $Pb(Zr,Ti)O_3$; PZT

1. Introduction

In recent years, there has been an increasing interest in ferroelectric thin films, in particular, those that present a perovskite-type crystalline structure, displaying also large values of spontaneous polarization. These materials are of great interest for a wide range of applications such as non-volatile memories, dynamic random access memories, solid state displays, infrared detectors, pyroelectric and piezoelectric sensors, microwave devices, electro-optic and integrated-optic devices.[1–4] The perovskite oxides, owing to their large values of spontaneous polarization, and to their simple crystal structure, are among the most studied ferroelectrics.[5–7]

Particular research interest has been devoted to lead zirconate titanate (PZT) thin films and powders, one of the most thoroughly investigated ferroelectric materials. $Pb(Zr,Ti)O_3$ is a solid solution of lead zirconate and lead titanate that presents important interest not only for basic science but also from the technological point of view.[8–11] This perovskite structured material presents ferroelectric properties at room temperature when its phase has a non-centrosymmetric structure, i.e. tetragonal, rhombohedral or orthorhombic.

Non volatile memories based on ferroelectric PZT thin film capacitors are very promising, because they exhibit a spontaneous polarization that can be reversed by an electric field. At zero field, there are two equally stable states of polarization, $+P_r$ and $-P_r$. This type of behavior enables a binary-state device in the form of a ferroelectric capacitor. With the advent of sophisticated thin-film deposition technologies, the field of ferroelectric PZT thin films have been attaining renewed enthusiasm and attention. Research and development efforts in many laboratories are focused on the preparation of these films. Standard methods of PZT thin film manufacture, such as sputtering techniques, laser

* Corresponding author. Fax: +55-16-2615215.
E-mail address: derl@power.ufscar.br (E.R. Leite).

0955-2219/03/$ - see front matter © 2003 Elsevier Ltd. All rights reserved.
doi:10.1016/S0955-2219(03)00318-2

ablation or chemical vapor deposition, often lead to difficulties in controlling the stoichiometry of multicomponent oxide systems. Lin et al.[12] have found that a serious asymmetry appeared in the hysteresis loop, when a voltage was applied across a PZT thin films prepared by pulsed laser deposition (PLD). Guerrero et al.[13] have prepared PZT thin films with $SrRuO_3$ bottom electrodes. X-ray diffraction measurements revealed that epitaxial heterostructures with a high crystalline quality were obtained. The measured ferroelectric parameters P_r and E_c were respectively 13 $\mu C/cm^2$ and 150 kV/cm.

On the other hand, the research of new routes for obtaining solutions for thin film deposition remains an interesting subject. The use of the chemical processes for thin film production allows the precise control of the chemical composition. Nowadays, new solution deposition methods, based on wet chemistry, have been used for the preparation of oxide thin films. In this regard, chemical processing using solutions, including soft solution processing, has been attracting increased interest. The soft solution processing can be defined as an environmentally friend processing, using aqueous solutions. It also seems to provide results similar to every other process which uses fluids such as vapor, gas, and plasma or beam/vacuum processing, while consuming less total energy than the other processing routes.

Additionally, one of the most important technological issues for soft solution processing is its integration with functional device technology. In other words, it is a process compatible with many semiconductor fabrication technologies. Among the several soft solution processing, the sol-gel method has been widely used for the preparation thin films different. However, in the sol-gel method, precursor solutions are usually water sensitive and tend to gel quickly, which imposes stability problems often suffer from chemical and phase heterogeneities in derived multicomponent gel. In addition, several sol-gel methods use 2-methoxyethanol as a reactant and solvent. However, some of the disadvantages of many of the available metal alkoxides in 2-methoxyethanol solvent for thin film preparation are their extreme reactivity toward atmospheric moisture and the differential hydrolysis and condensation kinetics in each individual metal compound. It is thus crucial to design a suitable precursor solution, which enables formation of a homogenous multicomponent gel without any phase segregation throughout the processing. Furthermore, handling the 2-methoxyethanol used as a solvent is quite dangerous. Handling this teratogenic solvent presents a safety concern. The soft solution processing known as polymeric precursor method[14–19] can be included in class sol-gel method. This method yields products with much higher homogeneity than does the solid-state processing. This technique is a very promising alternative for molecular-scale control of nanostructured materials and nanocomposite.[20] The basic idea behind the polymeric precursor methods is to reduce individualities of different metal ions, which can be achieved by encircling stable metal complexes with growing polymer nets. Immobilization of metal-complexes in such rigid organic polymeric networks can reduce the segregation of particular metals, thus ensuring the compositional homogeneity in a molecular-scale. This is of vital importance for the synthesis of multicomponent oxides (e.g. Pb, Zr, Ti, Ba, Sr) with complicated compositions, since the chemical homogeneity with respect to distribution of cations in an entire system of resine (gel) often determines the compositional homogeneity of the final complex mixed oxides. This method is specially useful for reducing processing costs and for allowing large-area fabrication and stoichiometric composition control. It is also very attractive to stack multiple coatings of different kinds of perovskite complex oxides over thin films

Considering that the polymeric precursors method has been successful in preparing some oxide thin films, this work reports on the preparation and characterization (morphology, phase and electrical properties) of PZT thin films based on a soft solution processing, the so-called polymeric precursor method.

2. Experimental

Lead (II) acetate trihydrate ($Pb(CH_3COO)_2.3H_2O$), 99% purity (Aldrich), Titanium (IV) isopropoxide ($Ti[OCH(CH_3)_2]_4$), 97% purity (Aldrich), zirconium-tetra-*n*-butoxide ($Zr(OC_4H_9)_4$), 98% purity (Aldrich), ethylene glycol ($HOCH_2CH_2OH$), 99 purity (J.T. Baker) and citric acid ($H_3C_6H_5O_7$) 99% purity (Mallinckrodt) were used as starting materials. $PbZr_{0.3}Ti_{0.7}O_3$ (PZT) thin films were deposited on Pt/Si substrates by the polymeric precursor method. Titanium citrate and zirconium citrate were formed by the dissolution of, respectively, titanium (IV) isopropoxide and zirconium-tetra-*n*-butoxide in water solutions of citric acid, under constant agitation. After homogenization of the solutions containing Ti and Zr, they were mixed in a molar proportion of 30:70 of zirconium and titanium, respectively. The citrate solution was well stirred for some hours at 60 °C to yield a clear and homogenous solution. Lead acetate trihydrate was dissolved in water, after then it was added in a stoichiometric quantity, to the titanium–zirconium citrate solution. Ammonium hydroxide was used to adjust the pH of the solution (pH 7–8) and to prevent precipitation of lead citrate, what is favored in an acid solution. After homogenization of the solution containing Pb in the cations, ethylene glycol was added to promote citrate polymerization by the polyesterification reaction. With continued heating at 80–90 °C, the solution became more viscous, albeit

devoid of any visible phase separation. The viscosity of the deposition solution was adjusted to 20 mPa.s by controlling the water content.

The evolution of the gel system with temperature was investigated by simultaneous thermogravimetric analysis (TGA) and differential scanning calorimetry (DSC) (STA 409, Netzsch, Germany), in synthetic air (30 cm^3/min) using a constant heating rate of 10 °C/min from room temperature up to 600 °C.

$Pt/Ti/SiO_2/Si$ wafers were used as substrates, which were spin-coated by dropping a small amount of the polymeric precursor solution onto them. Rotation speed and spin time were fixed at 6000 rpm and 30 s, respectively. After deposition, the layer was dried at 150 °C on a hot plate for 20 min to remove residual solvents. The heat treatment was carried out in two stages: initial heating at 400 °C for 2 h at a heating rate of 5 °C/ min to pyrolyze the organic materials, followed soon thereafter by heating at 500, 600 and 700° C for 2 h to crystallize the films. Each layer was pyrolyzed at 400 °C and crystallized at 500, 600 and 700 °C before the next layer was coated. This process was repeated several times to achieve the desired film thickness.

X-ray diffraction (XRD) patterns were obtained using a Cu K_α radiation source to determine the structure of the films in the θ–2θ scan mode, recorded on a Rigaku diffractometer, model D/max-2500/PC. The power conditions were 40 kV at 150 mA. The thickness of the coated film was measured by thin film cross-section analysis made by scanning electron microscopy (SEM), Zeiss DSM940A. Atomic force microscopy (AFM) was used to obtain a 3D image reconstruction of the sample surface. These images allow for an accurate analysis of the sample surface and the quantification of very important parameters such as roughness and grain size. A Digital Instruments Multi-Mode Nanoscope IIIa was used. The micro-Raman measurements were performed at room temperature in thin films, using the 514.5 nm line of an argon ion laser as the excitation source. The power was kept at 15 mW and a 100× lens was used. The spectra were recorded using a T-64 Jobin-Yvon triple-monochromator coupled to a CCD detector. Infrared analyses were performed by means of Equinox/55 (Bruker) Fourier Transformed Infrared (FTIR) spectrometer, equipped with a 30° specular reflectance accessory. The FTIR reflectance spectra of thin films were recorded at room temperature in the 350–1200 cm^{-1} frequency range, allowing to observe the lattice vibration of the thin films deposited at the different temperatures.

The dielectric and ferroelectric behavior of the PZT ($PbZr_{0.3}Ti_{0.7}O_3$) thin films was measured in the metal–PZT–metal configuration, with the films sandwiched between the bottom platinum and top gold electrodes. The Au top electrode area 3.1×10^{-4} cm^2 was deposited by sputtering through a designed mask onto the film surfaces. The ferroelectric hysteresis was determined using Radiant Technologies RT6000HVS ferroelectric test system. These loops were traced using the "charge" program included in the software of the RT6000HVS in a virtual ground mode test device. The capacitance–voltage (C–V) properties were measured using a Hewlett-Packard (4194A) impedance/gain phase analyzer, in which the capacitance value was taken using a small AC signal of 10 mV at 100 kHz. The dielectric constant and dissipation factor were measured as a function of frequency by using a frequency, in the 100 Hz–10 MHz range. The leakage current–voltage (I–V) characteristic was determined with a voltage source measuring unit (Keithley 237). All the measurements were taken at room temperature.

3. Results and discussions

3.1. Structure and microstructure

Fig. 1 shows the DSC–TGA curves in a synthetic air atmosphere for the decomposition of a gel sample and a pre-pyrolyzed powder. The thermogravimetric analysis (TGA curve) of the polymer shows about four decomposition stages. The TGA analysis indicated a major weight loss (40%) between 50 and 200 °C, what corresponds to the evaporation of absorbed water and other residual organics, followed by a weight loss (25%) between 250 and 500 °C, which is probably due to the drastic removal of carboxylic groups and their combustion. After 500 °C, no obvious weight loss was observed. To verify the crystallization peaks, pre-pyrolyzed powders of PZT (30/70) were calcined at 300 °C for 24 h to remove the organic materials. The TGA curve (Fig. 1b) shows a small weight loss of about 5%. Differential scanning calorimetry analysis carried out in the pre-pyrolyzed powder shows two overlapped exothermic peaks (466 and 502 °C) before 500 °C; no further changes beyond 550 °C were observed. After deconvolution, by

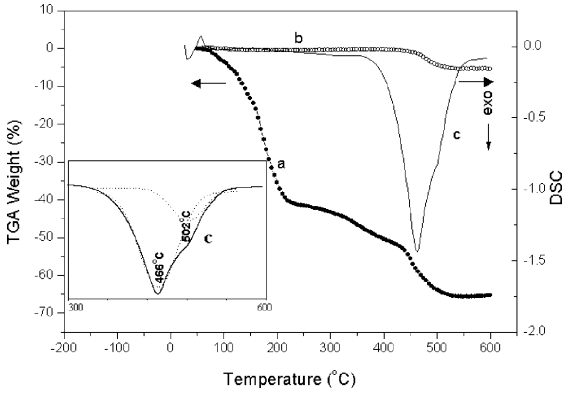

Fig. 1. DSC–TGA curves in a synthetic air atmosphere for: (a) TGA curve for gel sample; (b) TGA curve for pre-pyrolyzed powder; (c) DSC curve for pre-pyrolyzed powder. Inset details shown DSC curve.

fitting two gaussian curves, the maxima of the DSC peaks were determined to be at 466 and 502 °C, respectively, as shown in the insert of Fig. 1, reflecting two processes. The first process, with an exothermal peak at 466 °C can be attributed to the formation of the amorphous phase of PZT. The second process, with an exothermal peak at 502 °C, is attributed to the crystallization temperature of the perovskite phase, later confirmed by XRD and FTIR data.

The FTIR absorption spectra of the PZT thin films deposited at temperatures ranging from 400 to 700 °C are shown in Fig. 2. Measurements were carried out in the reflection mode. From the FTIR data of the PZT thin films heat-treated at various temperatures, it is revealed that at 400 °C, a broad absorption peaks of the BO_6 stretching mode, at 600–840 cm^{-1} obviously appears, suggesting the formation onset of BO_6 octahedra.[21] With increase in the heat-treated temperature, the absorption peaks at 389, 428 and 680 cm^{-1}, that are due to resonance with the longitudinal optic (LO) phonon modes become sharper and narrower, and they shift very slightly toward higher wavenumbers. This is considered to be a network stiffening and a structural rearrangement, which leads to the perovskite phase formation, increasing the crystallinity of the PZT thin films.[22,23]

The crystalline nature of the PZT thin film calcinated at various temperatures was studied by X-ray diffraction. As can be seen from Fig. 3, the film annealed at 400 °C was amorphous. As the annealing temperature was increased, the peaks in the XRD patterns became sharper and more intense, indicating better crystallinity. The XRD patterns also revealed that the films were polycrystalline with no evidence of preferred orientation or secondary phases, i.e. pyrochlore phase. The crystalline phase has a tetragonal structure, indicated by the presence of the (001/100) and (110/101) peaks. In addition, the tetragonal phase can be identified using Micro-Raman spectroscopy, as will be discussed later.

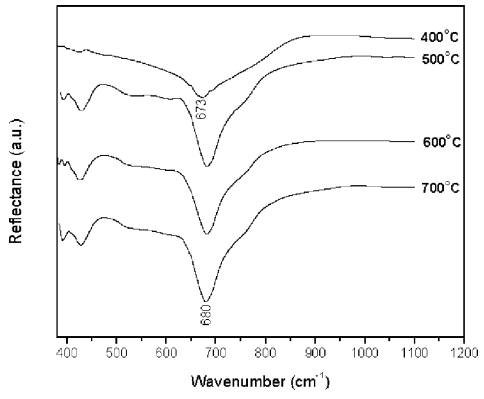

Fig. 2. FT-IR spectra of PZT 30/70 thin films annealed at to various temperatures.

The room temperature Micro-Raman spectra for PZT thin films annealed at different temperatures are shown in Fig. 4. The PZT thin film annealed at 400 °C maintains the amorphous nature. Annealing the thin films at higher temperatures results in the PZT perovskite phase developed with tetragonal structure. As a result, the Raman excitation of active modes becomes stronger and stronger, which is a good indication of the development of crystallinity for the PZT 30/70 perovskite phase. The peaks at wavenumber around 139, 203, 287, 341, 445, 498, 610 and 728 cm^{-1} are identified as A1(1TO), E(2TO), B1 + E, A1(2TO), E(2LO) + A(2LO), E(3TO), A1(3TO) and E(3LO) + A1(3LO), respectively. All the Raman modes are assigned, according to the results of Burns and Scott.[24] In addition, the Raman spectra of the thin films are similar to the results of Meng et al.[25]

The surface morphology of a PZT thin film was recorded by atomic force microscopy (AFM) as shown in Fig. 5. AFM imaging was carried out in the contact mode, using a triangular shaped 200-micron long cantilever with a spring constant of 0.06 N/m. The scanning rate varied from 1 to 2 Hz and the applied force from 10 to 50 nN, depending on the sample/tip interactions. The

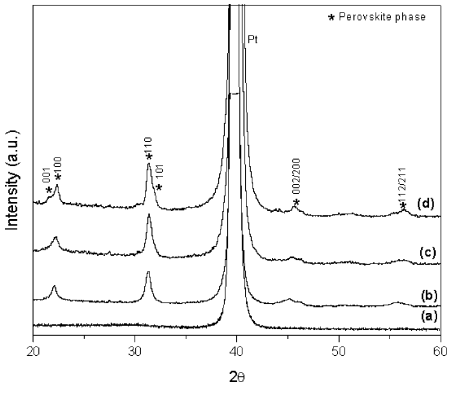

Fig. 3. XRD patterns of PZT 30/70 thin films annealed at various temperatures. (a) 400 °C; (b) 500 °C; (c) 600 °C and (d) 700 °C.

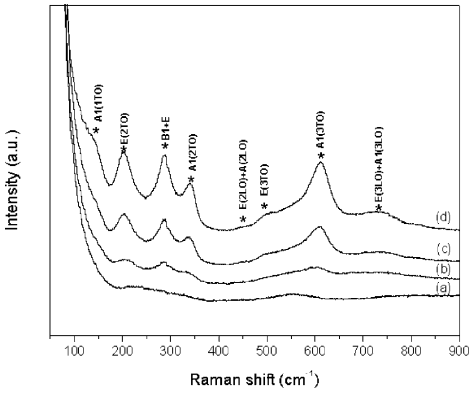

Fig. 4. Raman spectra at room temperature for PZT 30/70 thin films annealed at various temperatures. (a) 400 °C; (b) 500 °C; (c) 600 °C and (d) 700 °C.

surface roughness (rms) was measured using the equipment's software routine. It can be seen that the surface of the PZT thin film is smooth with densely packed grains, presenting a uniform microstructure without cracking and voids. No rosette structure, characteristics of the pyrochlore phase,[26] was observed. In addition, for thin films treated at temperatures below 700 °C (i.e. 500 and 600 °C), the PZT films did not exhibit rosette structures. The average grain size was about 150 nm, and the surface roughness was 2.4 nm. This value of roughness was lower than those for the PZT films prepared by sol-gel method[27] on $LaNiO_3/LaAlO_3$ and $LaNiO_3/SrTiO_3$ that had a roughness (rms) of 5.3 and 6.4 nm, respectively.

The scanning electron micrograph of the cross-section of a PZT thin film deposited on $Pt/Ti/SiO_2/Si$ substrate is shown in Fig. 6. From the cross-sectional profile shown in Fig. 6, the thickness of this thin film is approximately 365 nm.

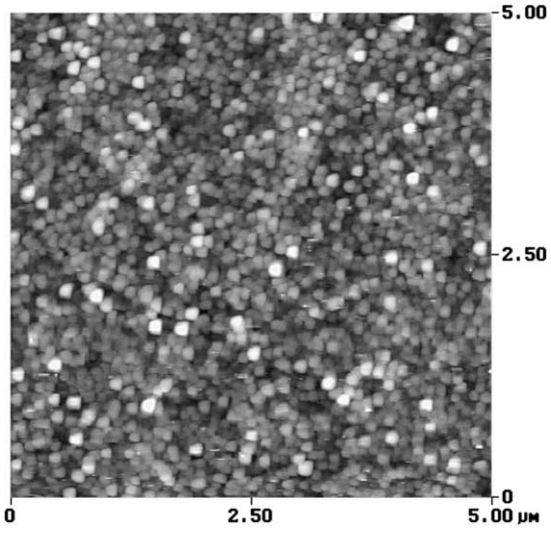

Fig. 5. AFM surface micrographs of a PZT thin film on $Pt/Ti/SiO_2/Si$ substrate, annealed at 700 °C for 2 h.

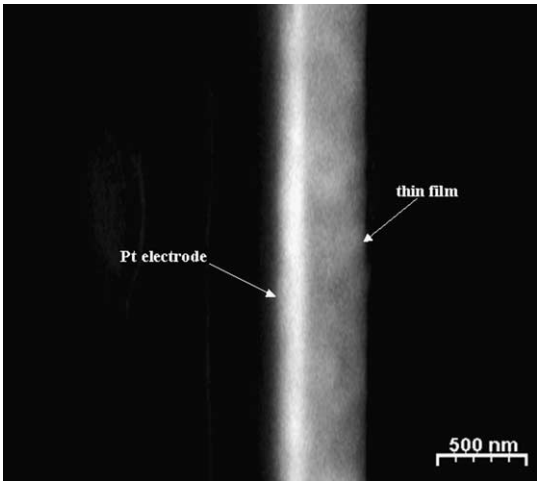

Fig. 6. Cross-sectional view of a PZT 30/70 thin film on $Pt/Ti/SiO_2/Si$ substrate, annealed at 700 °C for 2 h.

3.2. Electrical properties

Fig. 7 shows the dependence of dielectric constant and dielectric loss, measured at room temperature on the frequency, in the range from 100 Hz to 10 MHz for films deposited on $Pt/Ti/SiO_2/Si$ substrates and annealed at 700 °C. The dielectric properties at the different regions of the films varied within 2–3%, indicating the compositional homogeneity and the thickness uniformity of the films. The dielectric constant and dielectric loss (tan δ) were about 646 and 0.090, respectively, at 1 kHz. These values are very promising for high-density DRAM applications. It can be observed that the values of dielectric constant slightly decreased with the frequency up to 10 MHz. On the other hand, PZT thin films prepared by pulsed laser deposition on $LaAlO_3$ substrates showed that above 1MHz, the dielectric constant abruptly decreased to values close to zero.[13] Meng et al.[28] prepared PZT thin films on $LaNiO_3$-coated Si substrates, using a modified sol-gel method. The dielectric constant at the frequency of 10 kHz was about 700, however its variation as a function of the frequency was greater and decreased, above 1 MHz, to values of about 90. A dielectric constant of 558 was reported for PZT thin films of the same composition deposited on $Pt/Ti/Si_3N_4/SiO_2/Si$ substrates prepared by sol-gel process.[29] In addition, multilayer thin films of PZT/PT on the same substrates, prepared by sol-gel process[29] showed a lower dielectric constant of about 389.

In general, C–V curves based on low-signal (~10mV) measurements have been used for the assessment of ferroelectricity. Fig. 8 shows the changes of dielectric constant as a function of bias voltage at 100 kHz. A hysteresis loop was observed when the bias voltage was swept between positive and negative values. The dielectric

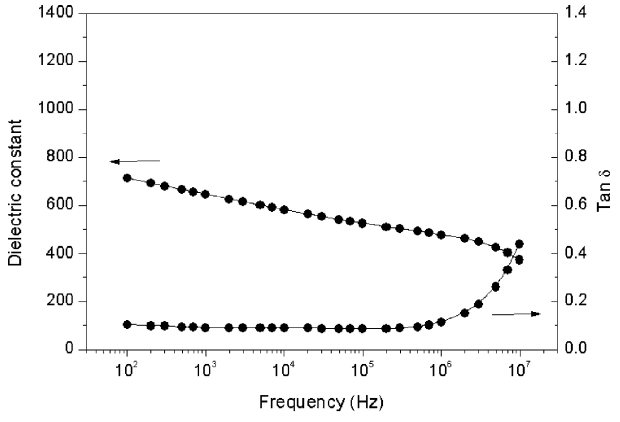

Fig. 7. The variation of dielectric constant and dielectric loss (tan δ) for the PZT thin films deposited on $Pt/Ti/SiO_2/Si$ substrates annealed at 700 °C.

constant dependence on the bias voltage and the presence of a hysteresis loop reflected the ferroelectric behavior of the PZT thin film at room temperature. The dielectric constant and dielectric loss for the films with 3.1×10^{-4} cm^2 electrode area obtained from C–V curves at zero bias, are about 567 and 0.11, respectively. It can be seen that the center of C–V curves is located at zero bias field, what suggests the absence of internal electric fields.[30] Their cause is due to space charge, asymmetric distribution of trapped charges, more specifically, trapped electrons, or charge accumulation at the interface between the thin film and the electrodes.[31] Also, the C–V curve displays symmetry in the maximum capacitance values that can be observed in the vicinity of the spontaneous polarization switching, showing the excellent quality of PZT thin films prepared by this method. On the other hand, PZT thin films prepared by LSMCD (liquid source misted chemical deposition) showed that the C–V curves were not symmetric along zero bias voltage, with the axis of symmetry shifted negatively.[32]

Polarizations versus voltage hysteresis loop were measured for the PZT thin films grown on Pt/Ti/SiO_2/Si substrates. Fig. 9 shows a typical hysteresis loop of a film annealed at 700 °C. Ferroelectricity was clearly confirmed. With the increasing electric field, the values of spontaneous polarization (P_s), remanent polarization (P_r) and coercive field (E_c) were increased. The measured values of $2P_s$, $2P_r$ and E_c from 200 to 440 kV/cm ranged from 70 to 136 μC/cm^2, 39 to 84 μC/cm^2 and 105 to 123 kV/cm, respectively, which were thought to correspond to good ferroelectric properties. The remanent polarization herein reported is superior to the value reported by Meng et al.[28] for PZT (30/70) thin films prepared by sol-gel process, the measured ferroelectric parameters P_r and E_c were respectively 20.5 μC/cm^2 and 31.6 kV/cm. Liu et al.[33] reported a modified solid precursor sol-gel process to prepare the PZT(30/70) thin films, the parameters P_r and E_c were respectively 20 μC/cm^2 and 100 kV/cm. Lee et al.[34] reported a sol-gel process where the precursor were synthesized by distilling and reflux in butoxyethanol to prepare the PZT thin films, the remanent polarization was 30 μC/cm^2. In addition, our values are comparable with PZT thin films obtained by other methods.[35–37]

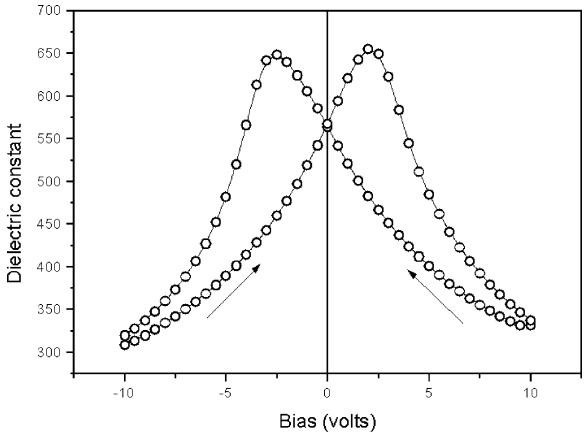

Fig. 8. The dependence of the dielectric constant of the PZT thin films annealed at 700 °C on the d.c. bias voltage.

A typical leakage current characteristic of PZT (30/70) thin films, measured with a voltage step of 0.1 V and elapsed time of 1.0 s for each voltage, is shown in Fig. 10. The top electrode was biased positively. Fig. 10 shows the measured current density (J) versus the electric field (E) in a log(J) vs log(E) plot for PZT thin films. It can be seen that there are two clearly different regions. The current density increases linearly with external electric field in the region of low electric field, what suggests an ohmic conduction. With increasing external field the current density increases exponentially, which implies that the current density is due to a Schottky or Poole–Frenkel emission mechanism. The leakage current density levels at 1.5 V were of 4.8×10^{-7} A/cm^2. Cho and Jeon[38] observed behavior similar to PZT thin films prepared by sol-gel process with leakage current density of 7.22×10^{-8} A/cm^2. In addition, Lee

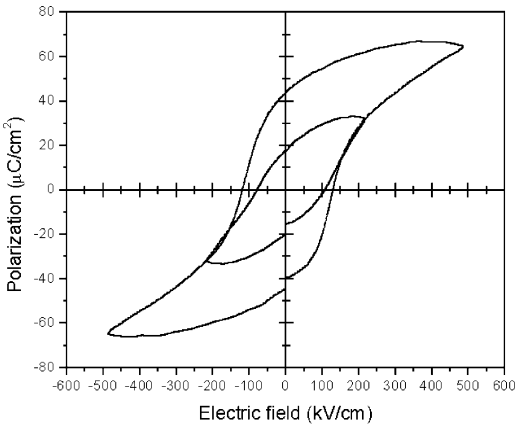

Fig. 9. P–E hysteresis loops for the PZT thin films annealed at 700 °C, measured at different electric fields.

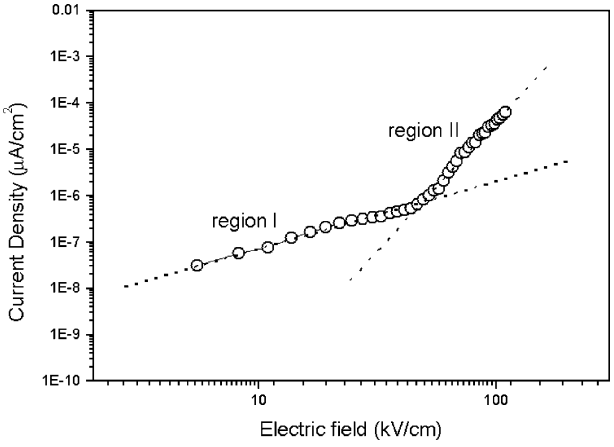

Fig. 10. Current–voltage characteristics for PZT thin film on Pt/Ti/SiO_2/Si.

and Joo[39] reported leakage current density of 1.1×10^{-7} A/cm^2 to PZT thin films prepared by radio-frequency magnetron sputtering using multimetal targets of Pb, Zr and Ti.

4. Conclusions

Spin-coated PZT (30/70) thin films were successfully grown onto Pt/Ti/SiO_2/Si substrates by the polymeric precursor method. The films were polycrystalline, single-phase perovskite, and had no preferential orientation identified by XRD data. In the FT-IR measurements, the BO_6 (B = Zr and Ti) metal–oxygen octahedral vibrational modes become stronger with the increase of the annealing temperature, suggesting the formation of the PZT perovskite phase. The Raman spectra undoubtedly show the PZT tetragonal phase of the thin films.

A smooth and dense surface with no rosette structure was observed by the AFM analysis. The surface morphology showed homogenous grains with an average size of 150 nm and a low surface roughness (rms 2.4 nm). The remanent polarization and coercive field were 44 μC/cm^2 and 123 kV/cm, respectively. The dielectric constant and dielectric loss (tan δ) at 1 kHz were 646 and 0.090, respectively, and the leakage current density at 1.5 V was about 4.8×10^{-7}A/cm^2. In addition, rosette structures that may lead to serious problems in the reliability of the FeRAM device were not found in the PZT thin films. Undoubtedly, the control of microstructure, in order to achieve a uniform grain structure is very important for the high quality of the thin film capacitor. As the $Pb(Zr_{0.3}Ti_{0.7})O_3$ thin films prepared by the polymeric precursor method (PPM) can meet the requirements, their electric properties are comparable with the properties of thin films obtained by other methods. Thus, this suggests that PPM can be an alternative to prepare PZT thin films with good electrical and microstructural qualities.

Acknowledgements

The authors gratefully acknowledge the financial support of the Brazilian financing agencies FAPESP, CNPq, PRONEX and CAPES.

References

1. Simon, M., Buse, K., Pankrath, R., Kratzig, E. and Freschi, A. A., Photoconductivity of photorefractive $Sr_{0.61}Ba_{0.39}Nb_2O_6$:Ce crystals at high light intensities. *J. Appl. Phys*., 1996, **80**(1), 251.
2. Kohli, M., Wuethrich, C., Brooks, K., Willing, B., Forster, M., Muralt, P., Setter, N. and Ryser, P., Pyroelectric thin-film sensor array. *Sensors Actuators*, 1997, **A60**(1–3), 147.
3. Bao, D., Wu, X., Zhang, L. and Yao, X., Preparation, electrical and optical properties of (Pb,Ca)TiO_3 thin films using a modified sol-gel technique. *Thin Solid Films*, 1999, **350**(1-2), 30.
4. Wu, D., Li, A., Ling, H., Yin, X., Ge, C., Wang, M. and Ming, N., Preparation of $(Ba_{0.5}Sr_{0.5})TiO_3$ thin films by solgel method with rapid thermal annealing. *Appl. Surf. Sci*., 2000, **165**(4), 309.
5. Zhang, W. F., Huang, Y. B. and Zhang, M. S., Optical properties of ferroelectric (Pb, La)(Zr, Ti)O_3 thin films grown by pulsed laser deposition. *Appl. Surf. Sci*., 2000, **158**(3-4), 185.
6. Rotter, L. D., Vaudin, M. D., Bonevich, J. E., Kaiser, D. L. and Park, S. O., Correlation of the optical gap of $(Ba,Sr)_yTiO_{2+y}$ thin films with film composition. *Thin Solid Films*, 2000, **368**(1), 41.
7. Kurogi, H., Yamagata, Y., Ebihara, K. and Inoue, N., Preparation of PZT thin films on YBCO electrodes by KrF excimer laser ablation technique. *Surface and Coating Technology*, 1998, **101**(1–3), 424.
8. Champeaux, C., Marchet, P. and Catherinot, A., Epitaxial ferroelectric PZT and BST thin films by pulsed UV laser deposition. *App. Surf. Sci*., 1996, **96-98**, 775.
9. Xue, J. M., Wang, J. and Weiseng, T., Synthesis of lead zirconate titanate from an amorphous precursor by mechanical activation. *Journal of Alloys and Compounds*, 2000, **308**, 139.
10. Kong, L. B., Zhu, W. and Tan, O. K., Preparation and characterization of $Pb(Zr_{0.52}Ti_{0.48})O_3$ ceramics from high-energy ball milling powders. *Mater. Lett*., 2000, **42**(4), 232.
11. Law, C. W., Tong, K. Y., Li, J. H. and Li, K., Leakage current in PZT films with sputtered RuOx electrodes. *Solid-State Electronics*, 2000, **44**(9), 1569.
12. Lin, Y., Zhao, B. R., Peng, H. B., Hão, Z., Xu, B., Zhao, Z. X. and Chen, J. S., Asymmetry in the hysteresis loop of $Pb(Zr_{0.53}Ti_{0.47})O_3/SiO_2$/Si structures. *J. Appl. Phys*., 1999, **86**(8), 4467.
13. Guerrero, C., Ferrater, C., Roldán, J., Trtík, V., Sánchez, F. and Varela, M., Epitaxial ferroelectric $PbZr_xTi_{1-x}O_3$ thin films for non-volatile memory applications. *Microelectronics Reliability*, 2000, **40**(4–5), 671.
14. Pechini, M. P., 1967, US Patent 3,330,697.
15. Pontes, F. M., Rangel, J. H. G., Leite, E. R., Longo, E., Varela, J. A., Araújo, E. B. and Eiras, J. A., Low temperature synthesis and electrical properties of $PbTiO_3$ thin films prepared by the polymeric precursor method. *Thin Solid Films*, 2000, **366**(1–2), 232.
16. Pontes, F. M., Longo, E., Rangel, J. H., Bernardi, M. I., Leite, E. R. and Varela, J. A., $Ba_{1-x}Sr_xTiO_3$ thin films by polymeric precursor method. *Mater. Lett*., 2000, **43**(5–6), 249.
17. Bouquet, V., Bernardi, M. I. B., Zanetti, S. M., Leite, E. R., Longo, E., Varela, J. A., Guilloux Viry, M. and Perrin, A., Epitaxially grown $LiNbO_3$ thin films by polymeric precursor method. *J. Mater. Res*., 2000, **15**(11), 2446.
18. Pontes, F. M., Araújo, E. B., Leite, E. R., Eiras, J. A., Longo, E., Varela, J. A. and Pereira-da-Silva, M. A., Microstructure and dielectric properties of (Ba,Sr)TiO_3 thin film produced by the polymeric precursor method. *J. Mater. Res*., 2000, **15**(5), 1176.
19. Pizani, P. S., Leite, E. R., Pontes, F. M., Paris, E. C., Rangel, J. H., Lee, E. J. H., Longo, E., Delega, P. and Varela, J. A., Photoluminescence of disordered ABO_3 perovskites. *Appl. Phys. Lett*., 2000, **77**(6), 824.
20. Leite, E. R., Carreño, N. L. V., Longo, E., Pontes, F. M., Barison, A., Ferreira, A. G., Maniette, Y. and Varela, J. A., Development of metal–SiO_2 nanocomposites in a single-step process by the polymerizable complex method. *Chem. Mater*., 2002, **14**, 3722.
21. Leite, E. R., Campos, C. M. G., Longo, E. and Varela, J. A., Influence of polymerization on the Synthesis of $SrTiO_3$. 1. Characteristics of the polymeric precursors and their thermal-decomposition. *Ceram. Int*., 1995, **21**(3), 143.
22. Zou, Q., Nourbakhsh, S. and Kim, J., Novel polyol-derived sol route for fabrication of PZT thin ferroelectric films. *Matt. Lett*., 1999, **40**, 240.

23. Verardi, P., Dinescu, M. and Cracium, F., Pulsed laser deposition and characterization of PZT thin films. *Appl. Surf. Sci.*, 2000, **154-155**, 514.
24. Burns, G. and Scott, B. A., Raman spectra of polycrystalline solids; application to the $PbTi_{1-x}Zr_xO_3$ system. *Phys. Rev. Lett.*, 1970, **25**, 1191.
25. Meng, J. F., Katiyar, R. S., Zou, G. T. and Wang, X. H., Raman phonon modes and ferroelectric phase transitions in nanocrystalline lead zirconate titanate. *Phys. Stat. Sol.*, 1997, **164**, 851.
26. Lu, W., Zhu, W. and Yao, X., Atomic force microscopic investigation of PZT thin films by MOD technology. *Ferroelectrics*, 1997, **196**(1-4), 337.
27. Cho, C. R., Heteroepitaxial growth and switching behaviors of PZT(53/47) films on $LaNiO_3$-deposited $LaAlO_3$ and $SrTiO_3$ substrates. *Mater. Sci. Eng.*, 1999, **B64**(2), 113.
28. Meng, X. J., Ma, Z. X., Sun, J. L., Bo, L. X., Ye, H. J., Guo, S. L. and Chu, J. H., Highly oriented $PbZr_{0.3}Ti_{0.7}O_3$ thin film on $LaNiO_3$-coated Si substrate derived from a chemical solution technique. *Thin Solid Films*, 2000, **372**(1-2), 271.
29. Liu, W. G., Ko, J. S. and Zhu, W. G., Preparation and properties of multilayer $Pb(Zr,Ti)O_3/PbTiO_3$ thin films for pyroelectric application. *Thin Solid Films*, 2000, **371**(1-2), 254.
30. Pontes, F. M., Leite, E. R., Longo, E., Varela, J. A., Araújo, E. B. and Eiras, J. A., Effects of the postannealing atmosphere on the dielectric properties of (Ba, Sr)TiO_3 capacitors: evidence of an interfacial space charge layer. *Appl. Phys. Lett.*, 2000, **76**(7), 2433.
31. Chen, H-m. and Lee, J.Y-m., Electron trapping process in ferroelectric lead–zirconate–titanate thin-film capacitors. *Appl. Phys. Lett.*, 1998, **73**(3), 309.
32. Moon, W. S., Woo, S. I. and Park, S. B., Preparation and characterization of lead zirconate titanate thin films by liquid source misted chemical deposition. *Thin Solid Films*, 2000, **359**(1), 77.
33. Liu, W., Ko, J. and Zhu, W., Influences of thin Ni layer on the electrical and absorption properties of PZT thin film pyroelectric IR sensors. *Infrared Physics & Technology*, 2000, **41**, 169.
34. Lee, E. G., Park, J. S., Lee, J. K. and Lee, J. G., Influence of annealing on the ferroelectric properties of $Pt/Pb(Zr,Ti)O_3/Pt$ thin film capacitors. *Thin Solid Films*, 1997, **310**, 327.
35. Cho, C. R., Francis, L. F. and Polla, D. L., Ferroelectric properties of solgel deposited $Pb(Zr,Ti)O_3/LaNiO_3$ thin films on single crystal and platinized-Si substrates. *Mater. Lett.*, 1999, **38**(2), 125.
36. Yan, F., Bao, P., Chan, H. L. W., Choi, C. L. and Wang, Y., The grain size effect of $Pb(Zr_{0.3}Ti_{0.7})O_3$ thin films. *Thin Solid Films*, 2002, **406**, 282.
37. Funakubo, H., Tokita, K., Oikawata, T., Aratani, M. and Saito, K., Comparison of crystal structure and electrical properties of tetragonaland rhombohedral $Pb(Zr,Ti)O_3$ films prepared at low temperature by pulsed-metalorganic chemical vapor deposition. *J. Appl. Phys.*, 2002, **92**, 5448.
38. Cho, S. M. and Jeon, D. Y., Effect of annealing conditions on the leakage current characteristics of ferroelectric PZT thin films grown by sol-gel process. *Thin Solid Films*, 1999, **338**, 149.
39. Lee, J-S. and Joo, S-K., The problems originating from the grain boundaries in dielectric storage capacitors. *Solid State Electronics*, 2002, **46**, 1651.